SOCIETY FOR SCIENCE AND EDUCATION
UNITED KINGDOM

AIVP ADVANCES IN
IMAGE AND VIDEO PROCESSING

A Imaging Supper-Resolution Processing Method for Effective Aperture Check of Thick Pinhole

Xie Hongwei Zhang Jianhua Zhang Faqiang Li Linbo Qi Jianmin
Institute of Nuclear Physics and Chemistry, China Academy of Engineering Physics, Mianyang, Sichuan, P.R. China, 621900

ABSTRACT

The Lucy-Richardson super resolution image processing technique, combined with the introduced virtual point spread function (PSF), was used to develop a measurement method of the processing precision of the superfine thick pinhole aperture. The principles of the technique were based on the known ideal image and degraded image. After the restoration and reconstruction of the degraded image with the introduced virtual point spread function (PSF)，the comparison is made between the reconstructed image and the ideal image to judge the correctness of the virtual point spread function (PSF). During this process, the simulation of the effects of the point spread function (PSF) upon the image reconstruction was carried out at first. As indicated by the simulation, the ideal point spread function (PSF) used in the image restoration and reconstruction could provide ideal results of the image reconstruction. However, in the case of relatively bigger size of the point spread function (PSF), the reconstructed image would be obtained smaller than the ideal image. Besides, related experiments were carried out on the cobalt radiation sources. In the experiments, the aperture of the shielded collimator to restrict and align the radiation source was known to be 1.0mm, the thick pinholes respectively 0.7mm and 0.45mm in aperture were used for the imaging of the Φ1mm radiation source, and the radiation image was recorded in imaging plates 0.05mm×0.05mm in spatial resolution. Based on the hypothesis that the processing precision of the thick pinhole fulfill the experiment requirements, the point spread function obtained from the simulated computation was introduced into the restoration and reconstruction of the recorded images. At the area with an intensity of 50%, the thick pinhole with 0.7mm aperture could provide homogenous image of the radiation source. However, the thick pinhole with 0.45mm aperture provided an elliptical image with a major-minor axis ratio of 5:3. The relatively big difference between the measurement results with the actual known object size indicates the relatively big gap between the virtual point spread function with the actual or real point spread function. This could be considered to be another indirect evidence of the relatively big difference between the actual processing precision of the 0.45mm aperture with the designed requirements.

Keywords: image super resolution, thick pinhole, Lucy-Richardson, neutron imaging

1. INTRODUCTION

During the inertial confinement fusion (ICF) experiments, the reacting conditions in the fusion thermal nucleus could be obtained from the diagnostics of information of high energy neutrons, γ-rays and other particles induced by the nuclear reaction in the D-T capsule. This attempt was succeeded in the laser-driven fusion [1]. At the same time, various diagnostic methods were well developed. As one of the major diagnostic methods, the pinhole photography was used to track

Xie Hongwei, Zhang Jianhua, Zhang Faqiang, Li Linbo and Qi Jianmin; *An Imaging Supper-Resolution Processing Method for Effective Aperture Check of Thick Pinhole*. Advances in Image and Video Processing, Volume 1, No 1, PP 01-09, (2013).
URL: http://scholarpublishing.org/index.php/AIVP/article/view/4/AIVP-13-1005
Publication Date: December 20th 2013

and record the spatial radiation flux of the high energy thermonuclear neutrons. This technique was considered to be a preferential option in terms of various aspects. Firstly, the flux could convey such important information of the implosion process more directly including the spatial scale, shape and homogeneity. Secondly, the spatial intensity distribution of neutrons with various energy levels could further reflect the temperature distribution in the target capsule. Thirdly, the spatial intensity distribution of the neutrons is independent on the surface density of the target capsule. Based on the above considerations, in the experiments, such diagnostic methods including the pinhole neutron imaging and penumbral imaging were developed to successfully obtain the profile images of the reacting area[2, 3].

Due to the fact that the size of the imaging aperture used in the penumbral imaging is a little bit bigger than that of the radiation source, the size of the radiation source could not be obtained directly. And the image information of the radiation source could only available after image processing. As for the case of the pinhole imaging, where the size of the imaging aperture is smaller than that of the radiation source, it could provide directly the size of the radiation source. However, due to the dependence of the spatial resolution largely upon the pinhole aperture, the relatively smaller size of the pinhole aperture could provide a fairly better spatial resolution but lacks in smaller neutron flux. Thus, as a common compromise, the requirement of the spatial resolution is lowered for the purpose of an acceptable sensitivity of the imaging recording system, as well as an acceptable impact of the detecting efficiency upon the image quality. The aperture of the thick imaging pinhole used in our ICF experiments were about 30μm[3], whose spatial resolution, in dealing with the radiation sources about 100μm in size, could not fulfill the experimental requirements. Thus, the super resolution image process of the existing neutron images was considered reasonably to be an important measure to obtain better image quality.

As a major parameter in the image reconstruction, the point spread function (PSF) is dependent on both the thick pinhole aperture and the material composition of the aperture. Besides, due to the relatively strong penetration effects of the neutrons, the PSF itself is dependent upon not only the size of the straight-throng area of the pinhole, but also upon the decaying maters in the pinhole materials. The shapes of the thick pinhole are majorly in circle, or triangle and square sometimes. Another major factor to affect the PSF size is the processing precision of the thick pinhole. Generally, the thick pinhole is made of such high density maters as tungsten (W), with a thickness of over 20cm, or even more than 50cm in the extreme conditions. As for the manufacturing procedure, the thick pinhole is assembled with segmented parts. Technically, it's very difficult to obtain experimentally the effective aperture of the superfine thick pinhole due to its relatively big total size.

In dealing with this issue, several options are available. The first option is to use laser diffraction method, where the processing precision could be provided based on the analysis of the configurations of the diffraction rings. This method could provide information mainly related with the shape of the aperture in the diffraction plane. Another option to detect the thick pinhole is CT

scanning with high energy γ-rays, which, however, could not provide satisfactory detecting precision for the experiment. In our past image reconstruction process of the super resolution of the neutron images, we used the simulated computational parameters based on an ideal thick pinhole[4]. Thus, in this paper, the super resolution image processing technique, combined with the introduction of the virtual point spread function (PSF), was used to develop a new measurement method of the processing precision of the superfine thick pinhole aperture.

2. PRINCIPLES OF THE DETECTION

2.1 Basic Principles of Thick Pinhole Imaging

Generally, the image of the radiation source is imaged and transmitted onto the image plane through the thick pinhole. And the intensity of the image plane could be given in the following equation:

$$g(x,y) = \iint h(x,y,x',y',f(x',y') \cdot f(x',y')dx'dy' \tag{1}$$

where: (x′,y′) is a point in the object plane, (x,y) is a point in the image plane, f(x′,y′) is the luminescence intensity at Point (x′,y′), and h(x,y,x′,y′,f(x′,y′)) is the corresponding intensity distribution of f(x′,y′) at Point (x,y) according to the imaging system characteristics. Suppose the image plane intensity is in the mode of the linear superposition, and based on its theory, the image plane intensity could be given as follows:

$$g(x,y) = \iint h(x,y,x',y')f(x',y') \cdot dx'dy' \tag{2}$$

where: h(x,y,x′,y′) is the response function at Point (x,y) in the image plane of Point (x′,y′) in the object plane. Again, suppose the response of f(x′,y′) to h is linear. The reason to make some hypothesis is to simplify the issues. Thus, based on the supposed ideal thick pinhole imaging process, and static object plane and image plane, the above equation could be alternatively expressed as follows:

$$g = h * f \tag{3}$$

However, the effects of the noise upon the system could never be excluded in the radiography. Consequently, the image plane intensity could be given in the following:

$$g = h * f + n \tag{4}$$

where: n is the noise of the recording system.

2.2 Rucy-Richardson Super Resolution Image Processing Method

R-L is actually a super resolution imaging processing method based Bayesin's theory, which could be expressed in the following[5,6]:

$$\hat{f}_{k+1}(x,y) = \hat{f}_{k}(x,y)\left[h(x,y) * \frac{g(x,y)}{\left| \hat{f}_{k}(x,y) h(x,y) \right|} \right] \tag{5}$$

where: $\hat{f}$ is the reconstructed image obtained after repeated commutation for k times. In the case of the experiment, based on the available h (the PSF of the system) and g (the recorded image), the reconstructed image could be obtained from iteration algorithm. And the reconstructed image is largely dependent on the PSF intensity distribution.

Things are quite different in the actual application, where, the PSF is unknown or even if known but with big uncertainty to result in a certain uncertainty for the image reconstruction. Fortunately, the effects of the PSF upon the super resolution image reconstruction could be analyzed by simulated computation. Firstly, the PSF in Gaussian distribution could be used to degrade the grid image. Then super resolution image reconstruction could be carried out according to Equation (5). The reconstruction results are given in Figure 1, where the image was reconstructed with ideal PSF, PSF with 2 pixels plus in size and PSF with 2 pixels minus in size, respectively. As indicated in this figure, with a relatively smaller PSF size, the reconstruction size is larger than the original size, while with relatively larger PSF size, the reconstruction size is smaller than the original size.

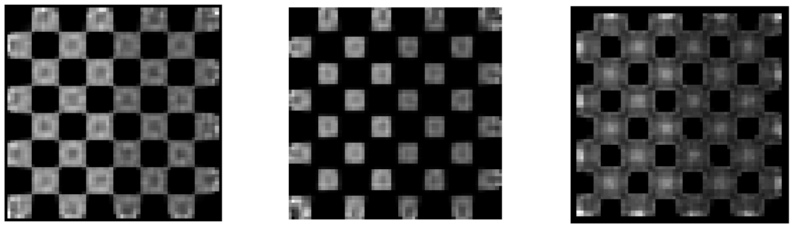

reconstructed with ideal PSF

reconstructed with PSF with 2 pixels plus in size

reconstructed with PSF with 2 pixels minus in size

Figure 1 : The R-L reconstruction results with different PSF sizes

The super resolution image reconstruction was made mainly based on the PSF of the image diagnostic system that was mainly obtained from such methods as precision measurement. In dealing with the case, where the original image is known, but the PSF uncertainty is relatively large or even with an unknown PSF, the following equation could be used for computation:

$$\hat{h}_{k+1}(x,y) = \hat{h}_{k}(x,y)\left[f(x,y) * \frac{g(x,y)}{\left| \hat{h}_{k}(x,y) f(x,y) \right|} \right] \tag{6}$$

As indicated by Equation (3), it could be roughly concluded that Equation (5) and Equation (6) are almost same but different in expression. Thus, after the shape of the original object and the degraded image produced by thick pinhole imaging are available or known, Equation (6) could be

used for the PSF computation of the thick pinhole imaging system. The same experimental results could also be obtained with Wiener super resolution image processing method. And the test results are basically same with those obtained from such traditional measurement methods such as the slit method and edge method.

3. EVALUAION METHODOLOGY

3.1 Experimental Setup

The experiment was made with 60Co radiation source with an intensity of 8.5×103Ci and a diameter of 30mm. A collimator with an aperture of about 1mm was placed 87.1cm away from the radiation source to provide shielding and beam restriction. The imaging thick pinhole was installed 114cm away from the collimating aperture. The image was recorded with the imaging plate, which was 197cm away from the thick pinhole. The amplification factor of the imaging system was 1.728, and the spatial resolution of the imaging plate was set to be 0.050mm/pixel.

3.2 Sensitivity Response of Imaging Plate

The imaging plate used in the experiment was provided by Fujifilm Medical Co. FCR PROFECT CS. The fluorescent reagent deliberately integrated in the imaging plate would be excited by the irradiation up to metastable state for the storage of the radiation energy. Such metastability, subject to a specific laser scanning, would be deexcited back to stable state same as that before irritation and transmit photons at the same time. The photon signals transmitted from all of pixels during deexcitation would be amplified with photomultiplier and converted in to digital signal output. Then the relationship between the image intensity and injected radiation flux could be determined by the data processing. As indicated by the experimental results, the dynamic rang of the imaging plate could be as large as up to 4 orders of magnitude. And the exposure time was appropriately determined in accordance with the relationships among the dynamic range, irradiation dosage and image intensity. In our experiment, the exposure time was set to be 1000s to provide a satisfactory signal-to-noise ratio (SNR) for the imaging system.

3.3 PSF of Thick Pinhole Imaging System

The PSF of the thick pinhole imaging system changes continuously with the change of the space. Generally, the PSF along the pinhole axis is used to interpret the spatial resolution of the thick pinhole imaging system[7]. The PSF of the thick pinhole imaging system could be obtained from the simulated computation. In dealing with a given thick pinhole, 6.5mm in material free path, 600mm in total length, 0.4mm in aperture, and 200mm in both object distance and image distance, the simulated computations of the PSF were carried out with various straight hole sections (30mm, 20mmand 10mm, respectively) and half angles of the conic strengthening segments at both ends (0.65°, 0.9° and 1.5°, respectively). The computational results are given in Figure 2. The PSF is consisting with transmittance component (the straight hole section) and the attenuation component through the pinhole matrix. And the attenuation component could be expressed by $\exp(-\mu L)$, where, μ is linear attenuation coefficient and L is the pass-throng thickness of γ-rays in the

attenuation matters. The amplification factor is the function of the PSF size, whose PSF could be given as r=D(1+M). In this equation, D is the pinhole diameter and M is the amplification factor.

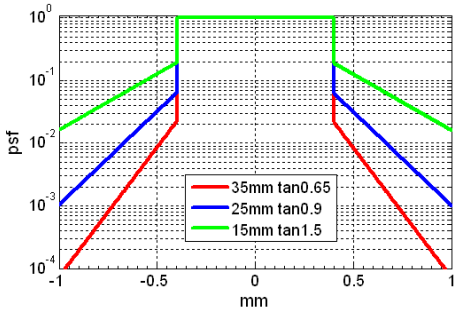

Figure 2: The structural diagram of the thick pinhole PSF

4. EXPERIMENTAL RESULT

During the experiment, a shielding collimator 1mm in aperture was used to provide beam restriction for the radiation source 30mm in diameter, as well as an equivalent radiation source Φ1mm in area. Then thick pinholes, 0.7mm and 0.45mm in aperture were used for imaging. With the laser beam as the benchmark, the collimator was aligned to be coaxial with the thick pinholes. The PSF along the pinhole axis is given in Figure 2. As for the thick pinhole with a straight hole section of 20mm, the effective clear aperture at 1% intensity attenuation would be expanded by about 0.1mm equaling to 2 pixel value. In this sense, the PSF of the ideal thick pinhole was used for the super resolution image reconstruction during the data processing.

The original image and reconstructed image obtained with 0.7m thick pinhole are given in Figure 3. As indicated in the figure, the reconstructed image is basically in circular, and the size at the 50% intensity is about 1mm. The original image and reconstructed image obtained with 0.45m thick pinhole are given in Figure 4. The reconstructed image is elliptical with a major-minor axis ratio of 5:3. Along the minor axis direction, the corresponding size at 50% intensity is about 1mm, indicating that this direction is corresponding to the 0.45mm pinhole thickness while the major axis direction is corresponding to the 0.7mm pinhole thickness.

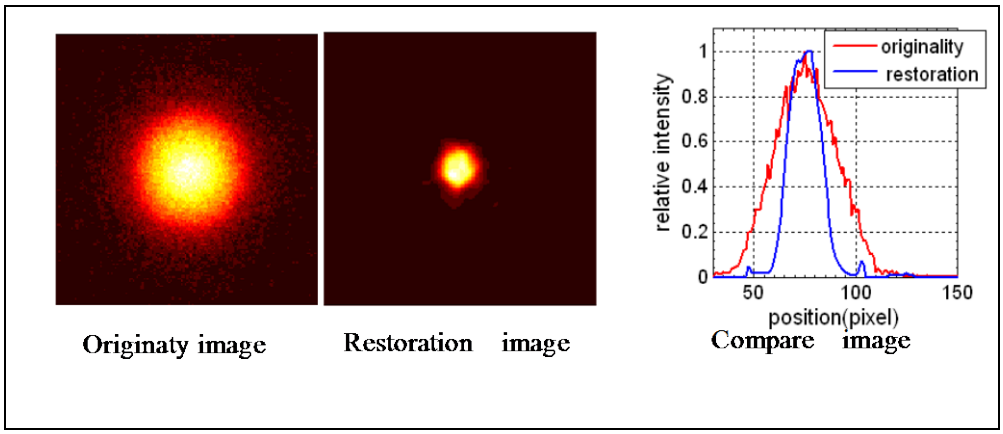

Figure 3 : The original image and reconstructed image obtained with 0.7m thick pinhole

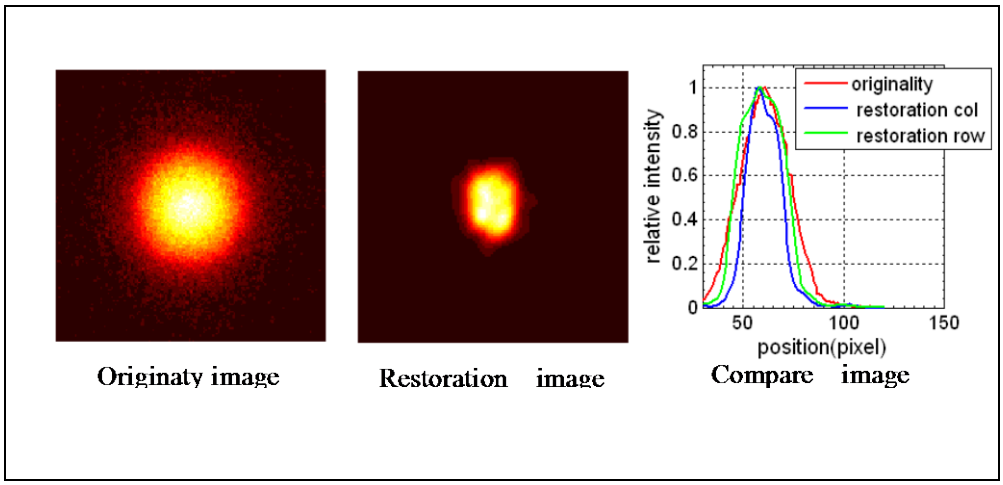

Figure 4 : The original image and reconstructed image obtained with 0.45m thick pinhole

5. DISCUSSION

5.1 Processing Precision of 1mm Thick Pinhole

During the processing of the superfine thick pinhole, the electrical discharge machining method was used to prepare a small pinhole aperture in about 0.2-0.3mm. Then, the low-speed wire grinding process on precise machine would be carried out to finish the fabrication of the thick pinhole. The precision of the product is dependent on the precision of the machine. Based on the confidence of the existing science and technology, the precision could presumably well fulfill the experimental requirements. During the experiment, the PSF of the 0.7mm thick pinhole was used for the super resolution image reconstruction. The size at 50% intensity was obtained to about 1.0mm and basically in circular shape. This could be considered as a roughly accordance of the hypothetical PSF of the thick pinhole with the ideal PSF, which provide an additional indirect evidence for the processing precision of the 0.7mm thick pinhole.

5.2 Processing Precision of 0.45mm Thick Pinhole

The super resolution image reconstruction was made for the images obtained with 0.45mm thick pinhole. The perpendicular/horizontal size ratio was about 5:3 at 50% intensity. The measurement results obtained with 1mm thick pinhole was quite different from those with 0.7mm thick pinhole. In terms of the fact that there's one but only one real image, the processing precision of the 0.45mm thick pinhole would be concluded unacceptable for the design requirement.

5.3 Evaluation of Measurement Precision

Since the PSF of the thick pinhole imaging system is determined by D(1+1/M), the PSF should be a major cause for the image degradation. In the ideal conditions, after the super resolution image reconstruction, the maximum correction size would roughly equal to the PSF size. In addition, the minimum precision of the image restoration is determined by the spatial resolution of the image

recording system. Thus, the ultimate precision in our experimental measurement could be determined to be about 0.05mm.

5.4 Reasons for Why not to Apply This Method into PSF Computation of Thick Pinhole Imaging System Directly

In our experiment setup, a 1.0mm collimating aperture was indeed placed in front of the radiation source. However, the collimating aperture was 87.1cm away from the radiation source and 114cm away from the imaging aperture at the same time. In accordance with the pinhole imaging principles, the collimating aperture would be considered as a penumbral intensity distribution. Hypothetically, the ideal intensity of the object plane should be a homogenous transmittance. Actually, with this additional 1mm radiation collimator, the distribution in a 1mm area in the aperture could not be homogenous. Thus, the PSF could not be determined with Equation (6), because this equation is only available for the ideal image and recorded image with homogenous intensity.

5.5 Spatial Resolution of Imaging Plate

In the experiment, the imaging plate was used to record the radiation image, but the effects of the imaging plate on the image processing were excluded from the super resolution image reconstruction.

6. CONCLUSION

The major application of the superfine thick pinhole was dealing with the image diagnostics of the high energy neutrons and γ-rays. The super resolution image processing, combined with the virtual PSF, was used to develop a new measurement method for the precision of the thick pinhole aperture. This method is based on the known image of the original object. And the correctness of the virtual PSF would be determined based on the comparison of the reconstructed image and the original image.

In this paper, the simulated study was presented. After that, imaging process was made for a radiation source 1mm in effective size with thick pinholes respectively 0.7mm and 0.45mm in aperture (a 1mm aperture collimator was used to provide beam restriction for the radiation source). Then, the super resolution image reconstruction, combined with the virtual PSF, was used to measure the processing precision of the thick pinhole. As indicated theoretically and experimentally, this method is concluded to applicable, reliable and simplified, which could provide the effective PSF of the thick pinhole imaging system.

ACKNOWLEDGMENTS

The authors owe great gratitude to Mr. Quan Lin, associate professor of Laboratory of Intense Cobalt Radiation Source, Northwest Institute of Nuclear Technology, who has provided assistance for our experiment. Besides, we are also very thankful for Prof. Xu Zeping and Yang Jianlun, and Dr.

Chen Faxin for their advice and help for our experiment and study. This work is Sponsored by CEAP Sci. & Tech. Development Foundation (CAEP 2010B0103006，CAEP 2011B0103017) and National Natural Science Foundation of China (Contract No. 11005095,11305155).

REFERENCES

[1]. Ress D,Lerche R A, Eill R J, Neutron imaging of laser-fusion targets,Science,Vol.241,p956-958,1988.

[2]. Sommargren G E,Lerche R A, Neutron Imaging of ICF Target Plasmas, review of scientific instruments, Vol.74, No.3, p1832-1836, 2003.

[3]. C. R. Christensen, Cris W. Barnes, First results of pinhole neutron imaging for inertial confinement fusion, review of scientific instruments, Vol. 74, No.5 , p2690-2694, 2003.

[4]. S. D. Metzler, J. E. Bowsher, Analytic Determination of the Pinhole Collimator' Point-Spread Function and RMS Resolution With Penetration，IEEE TRANS ON MED IMAG VOL. 21, NO. 8, p878-887, 2002.

[5]. Sungchae Jeona, Gyuseong Choa,ea tl‘Determination of point spread function for a flat-panel X-ray imager', Nuclear Instruments and Methods in Physics Research A 563,167-171, 2006.

[6]. David A. Reimann, Hooly A. Jacobs, Use of wiener filtering in the measurement of the two dimensional modulation transfer function, SPIE Vol.3977，P670-680，2000.

[7]. Xie Hong wei, Thick pinhole design applied to high energy ϒ ray source radiographic diagnostics, Nuclear Electronics & Detection Technology, Vol.31 No.2, P143-147, 2011.